ACS APPLIED MATERIALS & INTERFACES

Research Article

Cite This: ACS Appl. Mater. Interfaces 2020, 12, 1877−1884

www.acsami.org

Polydopamine-PEG−Folic Acid Conjugate Film Engineered TiO_2 Nanotube Arrays for Photoelectrochemical Sensing of Folate Binding Protein

Bobo Fan, Qi Fan, Lulin Hu, Min Cui, Xueying Wang, Hongmin Ma,* and Qin Wei

Collaborative Innovation Center for Green Chemical Manufacturing and Accurate Detection, Key Laboratory of Interfacial Reaction & Sensing Analysis in Universities of Shandong, School of Chemistry and Chemical Engineering, University of Jinan, Jinan 250022, People's Republic of China

Supporting Information

ABSTRACT: Serum-soluble folate binding protein (FBP) is an important tumor marker, and the development of a simple biosensing method is highly needed. In this work, a photoelectrochemical (PEC) biosensor for the detection of FBP was proposed based on the construction of an antifouling interface and the unique ligand−protein recognition. The PEC sensing platform was prepared by the biomimetic polydopamine (PDA) coating on TiO_2 nanotubes arrays (NTAs). A significant PEC enhancement effect was obtained due to the macroporous structures. Excellent antifouling performance was achieved by conjugation of amino-group-terminated 8-arm poly(ethylene glycol) (PEG). The incorporation of folic acid (FA) retains the antifouling property and shows recognition abilities toward FBP. The fabricated PEC biosensor shows good analytical performance. The combination of ligand−protein recognition and a PEC antifouling interface provides a good consideration for the development of FBP biosensors.

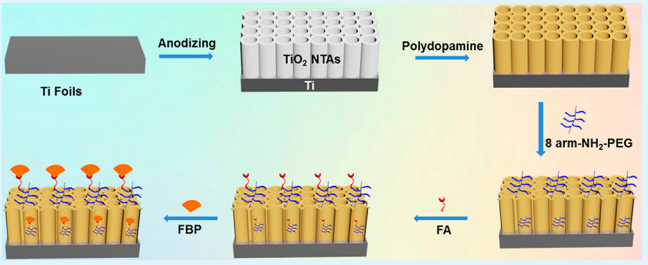

KEYWORDS: *folate binding protein, TiO_2 nanotubes arrays, folic acid, polydopamine, poly(ethylene glycol)*

1. INTRODUCTION

Folate binding protein (FBP), also called folate receptor (FR), is a membrane glycoprotein with a glycosyl-phosphatidylinositol tail. The membrane-associated FBP can be converted to a soluble form by metalloproteases.[1] Both the membrane-associated and the soluble forms of FBP show very high affinity with folic acid (FA).[2] FBP has been identified as a useful tumor marker because not only the overexpression on tissues and cells but also the elevated levels in serum are associated with several epithelial malignancies.[3−5] FA-mediated drug targeting has been well exploited for in vivo imaging and therapy of cancers and other diseases.[6−8] The unique ligand−protein interaction between FA and FBP has also been used in the field of in vitro diagnostics (IVD) for the detection of both free FBP and tumor cells in bodily fluids.[9,10] Ligand as a recognition element shows several advantages over traditional antibody−antigen interaction,[11] such as low cost and high stability. The easy conjugation of FA to materials or surfaces enables the development of various biosensing methods, including electrochemical,[12−14] electrochemiluminescence,[15,16] fluorescence,[17−19] colorimetric,[20,21] resonance Rayleigh scattering,[22] and photoelectrochemical (PEC)[23] methods. In spite of these achievements, a simple and robust biosensor for FBP with good performance is still needed in liquid biopsy of cancer.

PEC bioanalysis is promising and attractive because it inherits the high sensitivity, simple instrumentation, label-free response, and other advantages of the electrochemical method.[24] The easy availability of various semiconductor materials as PEC transducing elements enables the facile construction of sensing platforms with different performances.[25−27] TiO_2 nanotube arrays (NTAs) can be easily prepared by anodic oxidation of titanium and have been widely investigated in photocatalysis, solar cells, and water splitting.[28] TiO_2 NTAs have also been used for the construction of biosensing platforms due to the high porosity and large surface areas, which are favorable for the immobilization of recognition elements.[29] To improve the visible light response and conversion efficiency, semiconductor nanomaterials with narrow band gaps were usually used to form hybrids with TiO_2 NTAs.[30,31] Another issue for application in biosensing is the bioconjugation of TiO_2 NTAs with bimolecular recognition elements. Molecules with functional groups or metal nanoparticles should be used to modify TiO_2 NTAs before the immobilization of recognition molecules.[32] Previously we adopted the well-developed polydopamine (PDA) surface coating method for the construction of biosensing inter-

Received: September 28, 2019
Accepted: December 9, 2019
Published: December 9, 2019

DOI: 10.1021/acsami.9b17630
ACS Appl. Mater. Interfaces 2020, 12, 1877−1884

Scheme 1. Schematic Representation of the Fabrication of a PEC Biosensor for FBP Detection

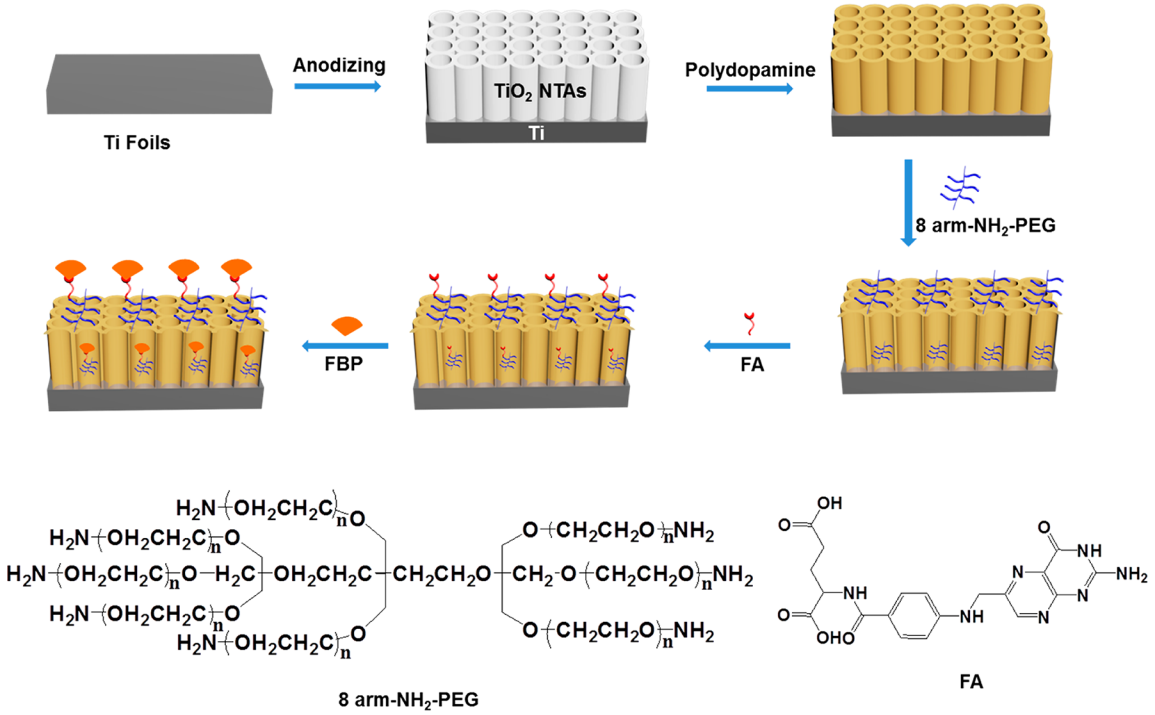

faces,[33,34] which can simultaneously solve the two issues above. However, the development of PDA-engineered TiO_2 NTAs for construction of biosensing interface is not well investigated.

While FA is a promising targeting molecule for drug delivery and cancer therapy, poly(ethylene glycol) (PEG)-FA conjugates have been widely prepared for the engineering of nanostructured vehicles.[35,36] PEGylation not only improves the solubility of the carriers but also more importantly prolongs the blood circulation time, which is a prerequisite for drug delivery.[37] The biocompatible, hydrophilic, and nonionic properties enable PEG also the most popular and successful molecule for the fabrication of an antifouling biosensing interface to decrease the nonspecific protein adsorption.[38,39] In this work, PEG−FA conjugates were used to engineer TiO_2 NTAs combined with the biomimetic PDA surface coating strategy.[40] The PDA-induced enhancement of PEC response is demonstrated to be more significant in the case of TiO_2 NTAs. A PDA−PEG−FA conjugate film engineered TiO_2 NTAs sensing platform shows good antifouling property and high recognition ability toward FBP.

2. EXPERIMENTAL SECTION

2.1. Materials and Reagents. Titanium foils (300 μm thick, 99.8%) were purchased from Sichuan Shengjili Industrial Co., Ltd. (Sichuan, China). TiO_2 nanoparticles (NPs), NH_4F, ethylene glycol (EG, 99.8%), tris(hydroxymethyl)aminomethane (Tris), dopamine hydrochloride (DA), and L-ascorbic acid (AA) were purchased from Shanghai Macklin Biochemical Co., Ltd. (Shanghai, China). Amino-group-terminated 8-arm poly(ethylene glycol) (NH_2−PEG, 10 K) was purchased from Jenkem Technology Co., Ltd. (Beijing, China). Bovine serum albumin (BSA) was obtained from Shanghai Aladdin Biochemical Technology Co., Ltd. (Shanghai, China). Immunoglobulin G (IgG) and hemoglobin (Hb) were purchased from Beijing Solarbio Science & Technology Co., Ltd. (Beijing, China). FR was purchased from Novoprotein Scientific Inc. (Shanghai, China). The serum was obtained from the Shandong Hospital of Traditional Chinese Medicine.

2.2. Apparatus. Scanning electron microscope (SEM) images were obtained using a field emission SEM (Zeiss, Germany). X-ray power diffraction (XRD) was acquired by a D8 advance X-ray diffractometer (Bruker AXS, Germany). JC2000D2G (Powereach, China) was used to measure the static water contact angle at differently modified electrodes. FTIR signals were measured by NICOLET iS10 (ThermoFisher Nicolet, America). The PEC and electrochemical impedance spectroscopy (EIS) measurements were tested at room temperature on the Zahner PEC workstation (Zennium-PP 211, Germany) using a conventional three-electrode system.

2.3. Preparation of TiO_2 NTAs/PDA and ITO/TiO_2 NPs/PDA Electrodes. The titanium foils were cut into 1 × 3 cm^2 pieces as a working electrode and then ultrasonically washed with ethanol, acetone, and ultrapure water separately for 30 min. Titanium pieces were anodized in EG containing 0.3 wt % NH_4F and 2% by volume H_2O at a constant voltage of 40 V to obtain highly ordered TiO_2 NTAs as described in the literature.[41] Two hours later, the resulting sample was calcined in a muffle furnace at 450 °C for 1 h. The prepared TiO_2 NTAs was soaked in the newly prepared DA solution (2×10^3 ng/mL) prepared with Tris-HCl buffer solution (pH = 8.5, 0.1 M). Two hours later, the electrode was washed by the Tris-HCl buffer solution. Finally, the TiO_2 NTAs/PDA electrode was prepared.

ITO glass is cut and cleaned in the same way as titanium pieces. TiO_2 NPs solution (10 μL, 5×10^3 ng/mL) was dropped onto the conductive surface of ITO glass and dried at room temperature. The resulting sample was calcined in a muffle furnace at 450 °C for 1 h to obtain the ITO/TiO_2 NPs electrode. Similarly, the ITO/TiO_2 NPs electrode was soaked in the newly prepared DA solution (2×10^3 ng/mL) for 2 h and rinsed with Tris-HCl buffer solution. Then the ITO/TiO_2 NTAs/PDA electrode was obtained.

2.4. Preparation of the PEC Biosensor. FA (25 mg) was dissolved in 2.5 mL of PBS (pH = 7.4) solution, and the pH of the solution was adjusted to 7.0 with NaOH (1 M). Then the EDC (11 mg) and NHS (16.5 mg) were added to the solution and stirred in the dark for 30 min. The solution was then stored at 4 °C away from light for one night.

First, the TiO_2 NTAs/PDA electrode was immersed into the NH_2−PEG soultion (1×10^3 ng/mL) prepared with Tris-HCl buffer solution for 0.5 h, as shown in Scheme 1. After being rinsed by the

DOI: 10.1021/acsami.9b17630
ACS Appl. Mater. Interfaces 2020, 12, 1877−1884

Tris-HCl buffer solution, the TiO_2 NTAs/PDA−PEG electrode was immersed in the FA solution. Thirty minutes later, the TiO_2 NTAs/PDA−PEG−FA electrode was rinsed by the PBS buffer solution, and then the TiO_2 NTAs/PDA−PEG−FA electrode was immersed in the FBP solution for 0.5 h at 4 °C for further use.

2.5. Investigation of the Antifouling Property of PEC Biosensor. To evaluate the antifouling property of the PEC biosensor, EIS and photocurrent changes of TiO_2 NTAs/PDA, TiO_2 NTAs/PDA−PEG, and TiO_2 NTAs/PDA−PEG−FA electrodes before and after BSA fouling were recorded, respectively. The EIS and PEC base responses of the electrodes immersed in the electrolyte solution (2.5 mM $K_3Fe(CN)_6$ and 0.1 M KCl for EIS, 0.1 M PBS with AA for PEC) were recorded, and then the EIS and photoelectric responses of the electrodes after soaking in PBS (pH = 7.4, 0.1 M) with 5×10^2 ng/mL BSA for 0.5 h were recorded. The same method was used to record the EIS and photoelectric responses of the TiO_2 NTAs/PDA−PEG electrodes after soaking in other interfering substances (IgG, Hb, and complex human serum) solutions. In order to further verify the antifouling ability of the TiO_2 NTAs/PDA−PEG−FA electrodes, the electrodes were immersed in BSA solutions of different concentrations (0, 0.05, 0.5, 5, 50, 5×10^2 ng/mL). To investigate the selectivity of the PEC biosensor for FBP, the TiO_2 NTAs/PDA−PEG−FA electrodes were immersed in FBP solution (1 ng/mL) and a mixed solution of FBP (1 ng/mL) and BSA (5×10^2 ng/mL), respectively. After 0.5 h, the electrode was rinsed with PBS, and then the PEC responses of the PEC biosensor were recorded. The frequency range of the EIS is from 0.1 Hz to 100 kHz. The wavelength of the excitation light source is 450 nm with a bias potential of 0.0 V.

2.6. Examination of PEC Biosensor for FBP Quantization Capability and Performance. Optimization of the experimental conditions, including the voltage and time of anodization and the concentration of the AA, DA, and PEG, is performed to give the PEC biosensor the best performance.

The TiO_2 NTAs/PDA−PEG−FA electrodes were immersed in the FBP solution with different concentrations (0.001−500 ng/mL) for 0.5 h. The PEC biosensor washed by PBS was tested three times, and the average was used to plot the working curve.

The photocurrent signal stability of the PEC biosensor was assessed by measuring the photocurrent of 12 consecutive switching lamps of the TiO_2 NTAs/PDA−PEG−FA electrodes modified with FBP (1 ng/mL). The PEC biosensor was then stored at 4 °C for 7 days to test its photocurrent response again to assess the storage stability of the PEC biosensor. The reproducibility of the PEC biosensor was investigated by measuring the photocurrent of five electrodes modified with FBP (1 ng/mL).

3. RESULTS AND DISCUSSION

3.1. Formation of PDA Coatings on TiO_2 NTAs. TiO_2 NTAs can be easily prepared by the anodizing method. However, the well-ordered TiO_2 NTAs are fragile and easily detached from the electrode (Figure S3A). Thus, the anodizing time and voltage were controlled to guarantee the stability of the prepared porous structures on electrodes. Under these conditions, TiO_2 NTAs are partially formed (Figure 1 A and 1C). The XRD characterization proves that the prepared TiO_2 NTAs are of anatase form (Figure S3B). The formation of PDA coating on TiO_2 NTAs can be confirmed by the color change of the electrodes from gray to yellow (Figure S2F). After the PDA coating, the skeletons of the porous structure become more smooth and protruding (Figure 1 B and 1D). As shown in Figure S3 C, the average thickness of the PDA film in the electrode is about 592.47 nm.

3.2. Enhancement Effect of PDA Coatings on the PEC Response of TiO_2 NTAs. We have previously shown that the PDA coating and the postprepared epinephrine−melanin can enhance the PEC response of the TiO_2 platform.[33]

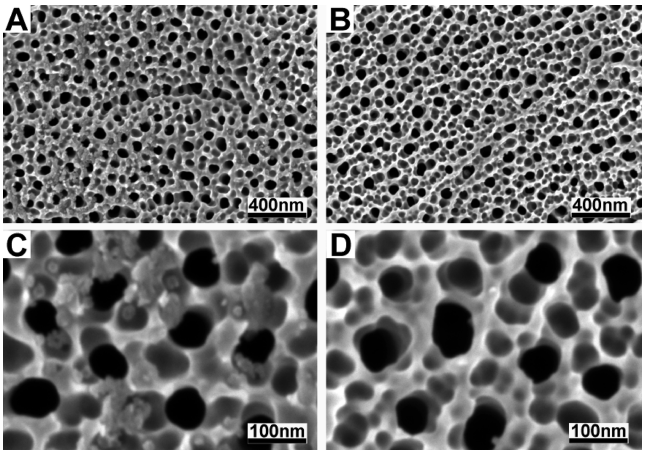

Figure 1. SEM images of TiO_2 NTAs (A and C) and TiO_2 NTAs/PDA (B and D).

Considering the macroporous structures of TiO_2 NTAs, better enhancement effects of PDA coatings are expected. To confirm this, TiO_2 NPs films on ITO were prepared (Figure S4) and were used as control electrodes for TiO_2 NTAs. Enhancement effects on PEC response are achieved for both TiO_2 NPs films and NTAs after the PDA coatings (Figure 2). Larger photocurrents are obtained due to the porous structures of TiO_2 NTAs over TiO_2 NPs films. The largest photocurrents are obtained at a coating time of 60 min. Under this coating time, about 3 times photocurrent increase (from 9.83 to 28.45 μA) is obtained for TiO_2 NPs films while nearly 6 times photocurrent increase (from 97.36 to 558.95 μA) is obtained for TiO_2 NTAs (Figure 2C). Obviously the enhancement effects of PDA coatings on PEC response are more significant in the case of TiO_2 NTAs. The larger photocurrent is beneficial for the development of sensing platforms with wide response ranges.

3.3. Grafting of PEG−FA Conjugates to PDA Coatings. The quinone structures in PDA films enable the facile grafting of molecules with amino groups through the Michael addition or Schiff base reaction.[42] The amino-group-terminated 8-arm PEG was first grafted to PDA film to construct an antifouling layer. The residual amino groups were designed as binding sites for further conjugation of FA as recognition elements. The successful incorporation of PEG and FA can be confirmed by the change of static water contact angles on the successively modified electrodes (Figure 3). The static water contact angle of titanium pieces was about (57.2 ±1.92)° (Figure S7). TiO_2 NTAs obtained by anodic oxidation showed good hydrophilicity,[43] and its static water contact angle was about (10.6 ±1.17)° (Figure 3A). The static water contact angle of the TiO_2 NTAs/PDA electrode interface was approximately (38.4 ±1.45)° (Figure 3B). With the modification of PEG with good hydrophilicity on the electrode, the static water contact angle of the TiO_2 NTAs/PDA−PEG electrode interface decreased to about (18.1 ±1.85)° (Figure 3C). When FA is modified on the TiO_2 NTAs/PDA−PEG electrode, the static water contact angle of the PEC biosensor interface is (25.7 ±1.24)° (Figure 3D). The presence of FTIR signals of the stretching vibration peak of the N−H bond at 3100−3200 cm^{-1} and the characteristic absorption peak of the carboxyl group appeared at 2786−2924 cm^{-1} further confirmed the incorporation of PEG and FA (Figure S10).

DOI: 10.1021/acsami.9b17630
ACS Appl. Mater. Interfaces 2020, 12, 1877−1884

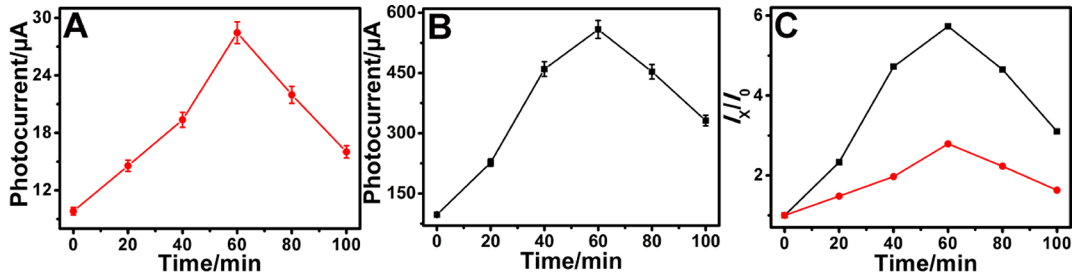

Figure 2. Photocurrents of TiO_2 NPs films on ITO (A) and TiO_2 NTAs (B) with different coating times of PDA. (C) Photocurrent ratio of TiO_2 (black curve, TiO_2 NTA; red curve, TiO_2 NPs) with different coating times (I_x) of PDA and TiO_2 modified without PDA (I_0).

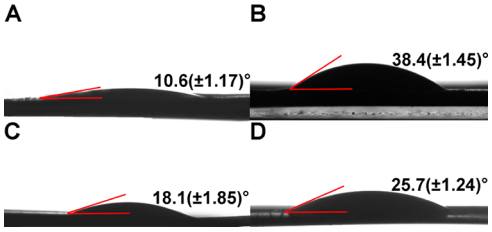

Figure 3. Static water contact angle of different electrode surface: TiO_2 NTAs (A), TiO_2 NTAs/PDA (B), TiO_2 NTAs/PDA−PEG (C), and TiO_2 NTAs/PDA−PEG−FA (D).

3.4. Antifouling Properties of the Fabricated PEC Sensing Interfaces. The antifouling ability of the PEC biosensor was investigated by comparing the EIS and photocurrent changes before and after BSA contamination. As shown in Figure 4A, the impedance spectrum includes the linear range with lower frequency and the semicircle with higher frequency equivalent to the electron transfer resistance (R_{et}). After the TiO_2 NTAs/PDA electrode is soaked in BSA solution, the R_{et} of the electrode increases greatly. This is because of the strong adhesion of PDA, which adsorbs BSA to the surface of the electrode and greatly hinders the electron transfer. However, as expected, there was little change in the R_{et} of the TiO_2 NTAs/PDA−PEG electrode before and after immersion in the BSA solution (Figure 4B). This is due to the strong hydrophilicity and steric repulsion effect of PEG, which makes it extremely difficult for BSA to be adsorbed on the surface of the TiO_2 NTAs/PDA−PEG electrode, so that the TiO_2 NTAs/PDA−PEG electrode has good antifouling ability. As can be seen from Figure 4C, after the TiO_2 NTAs/PDA−PEG−FA electrode was soaked by BSA solution, the R_{et} hardly changed. The results showed that the coupling of FA and PEG did not affect the antifouling ability of PEG, and the TiO_2 NTAs/PDA−PEG−FA electrode also had excellent antifouling ability.

Due to the attachment of the protein inhibiting the photocurrent of the PEC biosensor, changes in photocurrent can also be used to verify the antifouling ability of the electrode. As expected, the photocurrent was significantly reduced after the TiO_2 NTAs/PDA electrodes were soaked in the BSA solution (Figure 4D). The decrease in photocurrent at the electrode suggests that large amounts of BSA are adsorbed to the surface of the electrode. The photocurrent of the TiO_2 NTAs/PDA−PEG electrode (Figure 4E) and TiO_2 NTAs/PDA−PEG−FA electrode (Figure 4F) hardly changes after being soaked in BSA solution. This is because the PEC biosensor has good antifouling ability, and almost no BSA is adsorbed to the surface of the electrode. EIS and photocurrent have proved that the TiO_2 NTAs/PDA−PEG−FA electrode has excellent antifouling ability.

The antifouling performance of the PEC biosensor was further evaluated with the other common proteins (IgG and Hb) and human serum. The results based on EIS and photocurrent prove that the PEC biosensor has excellent antifouling ability for IgG (Figure S11A and S11D) and Hb

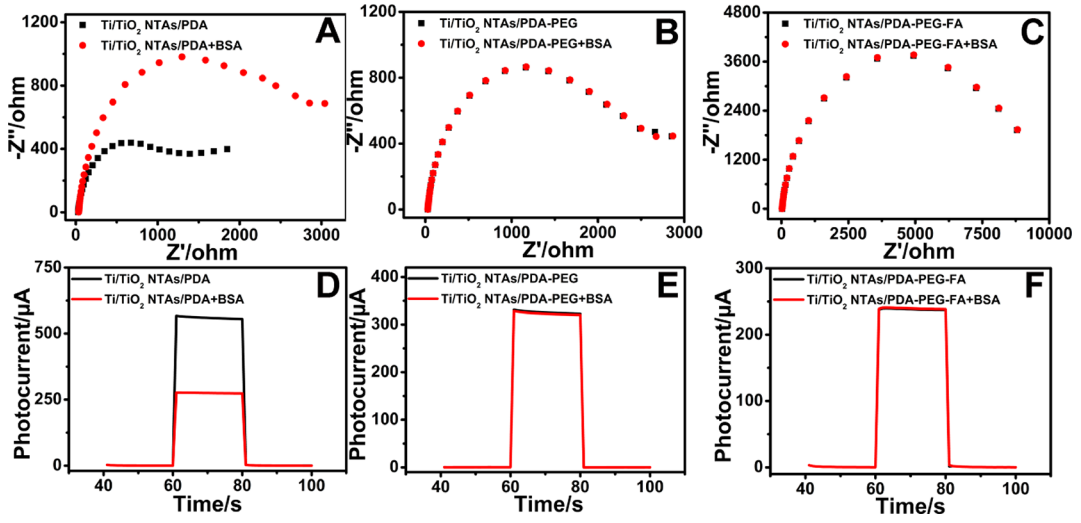

Figure 4. EIS and photocurrent responses of the different electrodes before (black curve) and after (red curve) soaking in BSA solution (5×10^2 ng/mL): TiO_2 NTAs/PDA (A and D), TiO_2 NTAs/PDA−PEG (B and E), and TiO_2 NTAs/PDA−PEG−FA (C and F).

DOI: 10.1021/acsami.9b17630
ACS Appl. Mater. Interfaces 2020, 12, 1877−1884

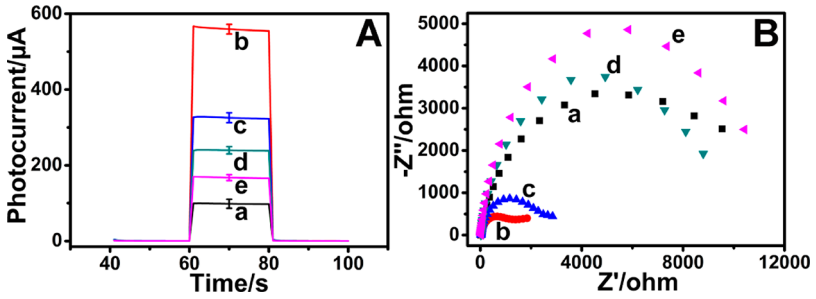

Figure 5. Photocurrent responses (A) and Nyquist plots of EIS (B) of the different modified electrodes: TiO_2 NTAs (a), TiO_2 NTAs/PDA (b), TiO_2 NTAs/PDA−PEG (c), TiO_2 NTAs/PDA−PEG−FA (d), and TiO_2 NTAs/PDA−PEG−FA/FBP (e).

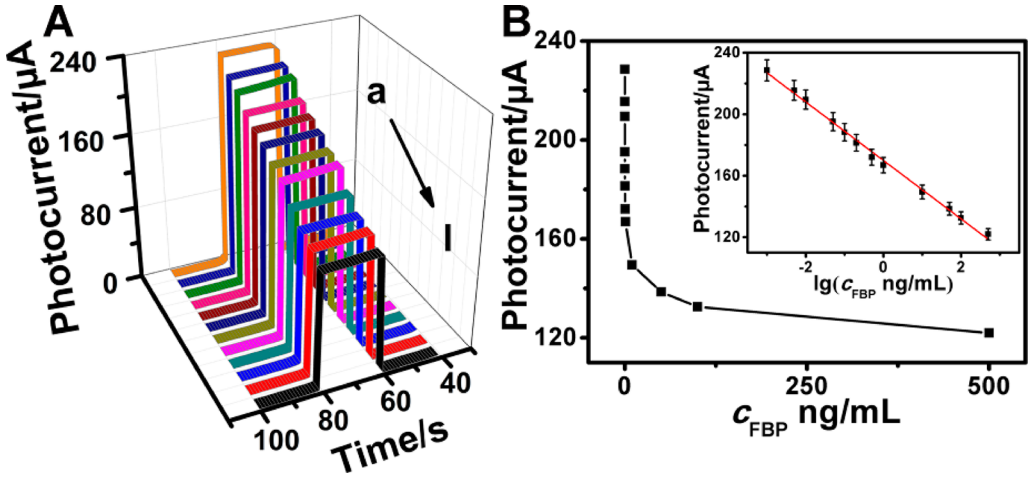

Figure 6. (A) Photocurrent of biosensors modified with different concentrations of FBP (a-l): 1×10^{-3}, 5×10^{-3}, 1×10^{-2}, 5×10^{-2}, 0.1, 0.2, 0.5, 1, 10, 50, 1×10^2, and 5×10^2 ng/mL. (B) Change in photocurrent with increasing FBP concentration from 1×10^{-3} to 5×10^2 ng/mL. (Inset) Linear relationship between the photocurrent and the logarithm of the FBP concentration.

(Figure S11B and S11E). After the TiO_2 NTAs/PDA−PEG−FA electrode was soaked in undiluted serum (Figure S11C and S11F), R_{et} increased by only 8.16% and photocurrent decreased by 4.21%. The results show that the PEC biosensor has good antifouling ability for complex system.

As shown in Figure S12, after soaking in different concentrations of BSA solutions (0, 0.05, 0.5, 5, 50, and 5×10^2 ng/mL), the photocurrent of the TiO_2 NTAs/PDA−PEG−FA electrode is almost the same, which proves that the biosensor has good antifouling ability.

3.5. PEC Response Based on the Ligand−Protein Interaction. In order to verify the feasibility of the PEC biosensor for FBP detection photocurrent was measured and compared during the construction of the PEC biosensor (Figure 5A). Due to the excellent photoelectric properties of TiO_2 NTAs, the photocurrent of THE TiO_2 NTAs electrode (curve a) is about 97.36 μA. The photocurrent of the electrode increased significantly after the PDA coating (curve b).When PEG (curve c) and FA (curve d) were successively modified to the electrodes, the photocurrent of the electrodes gradually decreases. This is because the introduction of PEG and FA hindered the reaction between AA and the photoinduced holes. When FBP is specifically bound to the TiO_2 NTAs/PDA−PEG−FA electrode by FA, the photocurrent of the electrode is further reduced (curve e).

In order to further verify the possibility of successful PEC biosensor construction, the process of PEC biosensor construction was further studied through EIS. As shown in Figure 5B, the TiO_2 NTAs electrode (curve a) has a large R_{et} due to the properties of semiconductor materials. When PDA is modified on the surface of the TiO_2 NTAs electrode, R_{et} of the TiO_2 NTAs/PDA electrode (curve b) decreases greatly compared to that of the TiO_2 NTAs electrode, which is related to the charge transfer of the PDA.[44] As PEG (curve c) and FA (curve d) are coated one by one on the electrode surface, the R_{et} gradually increases due to their weak conductivity. When FBP is adsorbed to the TiO_2 NTAs/PDA−PEG−FA electrode through the recognition of FA, the TiO_2 NTAs/PDA−PEG−FA/FBP electrode (curve e) has a relatively large R_{et} due to the poor conductivity of the FBP. The above results prove that the design scheme of the PEC biosensor construction proposed by us is feasible.

3.6. Quantitative Determination of FBP. Under optimal experimental conditions, the established PEC biosensor was used to quantitatively detect FBP at different concentrations (from 1×10^{-3} to 5×10^2 ng/mL). As shown in Figure 6A, as the concentration of modified FBP increases, the photocurrent of the PEC biosensor decreases gradually. This shows that the PEC biosensor we built can quantify FBP. As shown in Figure 6B, there is a good linear relationship between the photocurrent of the PEC biosensor and the logarithm of the FBP concentration at a FBP concentration from 1×10^{-3} to 5×10^2 ng/mL. The linear equation is $I = -18.99 \lg c + 169.96$ (R^2 = 0.996, c equals the concentration of FBP), and the detection limit (S/N = 3) is 2×10^{-4} ng/mL.

3.7. Selectivity, Stability, and Reproducibility of the PEC Biosensor. The selectivity, stability, and reproducibility are three important factors that affect the PEC biosensor

DOI: 10.1021/acsami.9b17630
ACS Appl. Mater. Interfaces 2020, 12, 1877−1884

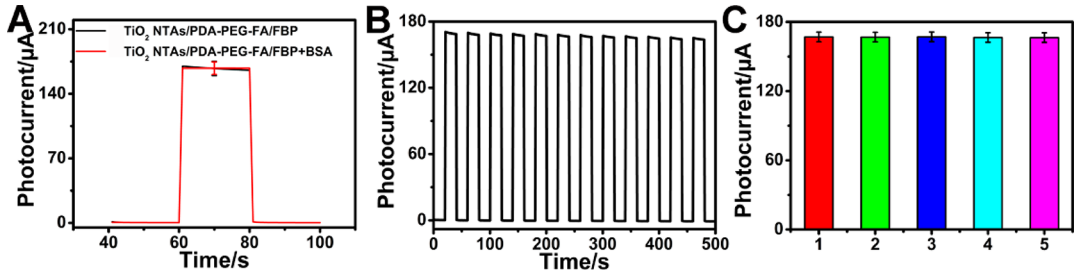

Figure 7. (A) Photocurrent of the TiO_2 NTAs/PDA−PEG−FA electrodes soaking in FBP solution (1 ng/mL) (black curve) and mixed solution (red curve) of FBP (1 ng/mL) and BSA (5×10^2 ng/mL). (B) Photocurrent of the TiO_2 NTAs/PDA−PEG−FA electrode modified with FBP (10 ng/mL) within 500 s. (C) Five photocurrents of the TiO_2 NTAs/PDA−PEG−FA electrode modified with FBP (1 ng/mL).

performance. The selectivity of the PEC biosensor to FBP was studied by comparing the photocurrent of the PEC biosensor in the FBP solution and the mixed solution. As shown in Figure 7A, the photocurrent of the PEC immersed in the single solution and the mixed solution is almost the same, which indicates that the PEC biosensor has good selectivity. It can be seen from Figure 7B that the PEC biosensor has good output signal stability, the photocurrent is relatively stable, and the relative standard deviation (RSD) of the photocurrent within 500 s is 1.13%. The photocurrent from the PEC biosensor after 1 week of storage was about 96.17% of the initial photocurrent. The RSD of the photocurrent of the five different PEC biosensors is 0.16% (Figure 7C). The results show that the PEC biosensor has good performance.

3.8. Real Sample Analysis. The recovery of FBP in serum samples was tested to investigate the ability of PEC biosensors to analyze actual samples. As shown in Table S3, the recovery rates of FBP with different concentrations were 99.33−101.03% and RSD was 2.04−3.10.

4. CONCLUSIONS

TiO_2 NTAs was obtained by anodic oxidation, and PDA−PEG−FA conjugate film was engineered onto TiO_2 NTAs. Compared with TiO_2 NPs, PDA can sensitize TiO_2 NTAs to a greater extent and increase TiO_2 NTAs photocurrent to improve the sensitivity of the PEC biosensor. PEG and FA greatly improve the specificity of the PEC biosensor. Therefore, the PEC biosensor we built has a wide detection range (from 1×10^{-3} to 5×10^2 ng/mL) and a low detection limit (2×10^{-4} ng/mL). This PEC biosensor construction method based on signal amplification strategy, ligand, and biomarker relationship provides a new idea for the method of PEC biosensor construction. At the same time, the PEC biosensor has excellent specificity and sensitivity, which makes it have broad prospects in clinical application.

■ ASSOCIATED CONTENT

Supporting Information

The Supporting Information is available free of charge at https://pubs.acs.org/doi/10.1021/acsami.9b17630.

Optimization of PEC biosensor construction conditions and detection conditions, photographs of TiO_2 NTAs and TiO_2 NTAs/PDA electrode, XRD pattern of the TiO_2 NTAs, static water contact angle of Ti piece, FTIR spectra of PEG−FA and TiO_2 NTAs/PDA−PEG−FA, EIS and photocurrent of the antifouling tests with IgG, Hb, and serum as interferers, static water contact angles values of different electrodes, photocurrent and R_{et} values of different electrodes, and comparison of this method with other methods (PDF)

■ AUTHOR INFORMATION

Corresponding Author

*Fax: (86) 531 82765969; Tel: (86) 531 82760510; E-mail: mahongmin2002@126.com.

ORCID

Hongmin Ma: 0000-0002-7061-8944

Qin Wei: 0000-0002-3034-8046

Notes

The authors declare no competing financial interest.

■ ACKNOWLEDGMENTS

This study was financially supported by the National Natural Science Foundation of China (21675063), the National Key Scientific Instrument and Equipment Development Project of China (No. 21627809), and the Jinan Scientific Research Leader Workshop Project (2018GXRC024).

■ REFERENCES

(1) Elwood, P. C.; Deutsch, J. C.; Kolhouse, J. F. The Conversion of the Human Membrane-Associated Folate Binding Protein (Folate Receptor) to the Soluble Folate Binding Protein by a Membrane-Associated Metalloprotease. *J. Biol. Chem.* **1991**, *266* (4), 2346−2353.

(2) Elwood, P. C.; Kane, M. A.; Portillo, R. M.; Kolhouse, J. F. The Isolation, Characterization, and Comparison of the Membrane-Associated and Soluble Folate-Binding Proteins from Human KB Cells. *J. Biol. Chem.* **1986**, *261* (33), 15416−15423.

(3) Toffoli, G.; Cernigoi, C.; Russo, A.; Gallo, A.; Bagnoli, M.; Boiocchi, M. Overexpression of Folate Binding Protein in Ovarian Cancers. *Int. J. Cancer* **1997**, *74* (2), 193−198.

(4) Campbell, I. G.; Jones, T. A.; Foulkes, W. D.; Trowsdale, J. Folate-Binding Protein is a Marker for Ovarian Cancer. *Cancer Res.* **1991**, *51* (19), 5329−5338.

(5) Henne, W. A.; Doorneweerd, D. D.; Lee, J.; Low, P. S.; Savran, C. Detection of Folate Binding Protein with Enhanced Sensitivity Using a Functionalized Quartz Crystal Microbalance Sensor. *Anal. Chem.* **2006**, *78* (14), 4880−4884.

(6) Low, P. S.; Henne, W. A.; Doorneweerd, D. D. Discovery and Development of Folic-Acid-Based Receptor Targeting for Imaging and Therapy of Cancer and Inflammatory Diseases. *Acc. Chem. Res.* **2008**, *41* (1), 120−129.

(7) Chen, H.; Li, S.; Li, B.; Ren, X.; Li, S.; Mahounga, D. M.; Cui, S.; Gu, Y.; Achilefu, S. Folate-Modified Gold Nanoclusters as Near-Infrared Fluorescent Probes for Tumor Imaging and Therapy. *Nanoscale* **2012**, *4* (19), 6050−6064.

(8) Stella, B.; Arpicco, S.; Peracchia, M. T.; Desmaële, D.; Hoebeke, J.; Renoir, M.; D'Angelo, J.; Cattel, L.; Couvreur, P. Design of Folic Acid-Conjugated Nanoparticles for Drug Targeting. *J. Pharm. Sci.* **2000**, *89* (11), 1452−1464.

DOI: 10.1021/acsami.9b17630
ACS Appl. Mater. Interfaces 2020, 12, 1877−1884

(9) Zheng, T.-T.; Zhang, R.; Zou, L.; Zhu, J.-J. A Label-Free Cytosensor for the Enhanced Electrochemical Detection of Cancer Cells Using Polydopamine-Coated Carbon Nanotubes. *Analyst* **2012**, *137* (6), 1316−1318.
(10) Weng, J.; Zhang, Z.; Sun, L.; Wang, J. A. High Sensitive Detection of Cancer Cell with a Folic Acid-Based Boron-Doped Diamond Electrode Using an AC Impedimetric Approach. *Biosens. Bioelectron.* **2011**, *26* (5), 1847−1852.
(11) Zhang, R.; Rejeeth, C.; Xu, W.; Zhu, C.; Liu, X.; Wan, J.; Jiang, M.; Qian, K. Label-Free Electrochemical Sensor for CD44 by Ligand-Protein Interaction. *Anal. Chem.* **2019**, *91* (11), 7078−7085.
(12) Cao, Y.; Zhu, S.; Yu, J.; Zhu, X.; Yin, Y.; Li, G. Protein Detection Based on Small Molecule-Linked DNA. *Anal. Chem.* **2012**, *84* (10), 4314−4320.
(13) Wang, H.-B.; Zhang, H.-D.; Xu, S.-P.; Gan, T.; Huang, K.-J.; Liu, Y.-M. A Sensitive and Label-Free Electrochemical Impedance Biosensor for Protein Detection Based on Terminal Protection of Small Molecule-Linked DNA. *Sens. Actuators, B* **2014**, *194*, 478−483.
(14) Ni, J.; Wang, Q.; Yang, W.; Zhao, M.; Zhang, Y.; Guo, L.; Qiu, B.; Lin, Z.; Yang, H.-H. Immobilization Free Electrochemical Biosensor for Folate Receptor in Cancer Cells Based on Terminal Protection. *Biosens. Bioelectron.* **2016**, *86*, 496−501.
(15) Li, R.; Wang, C.; Hu, Y.; Zheng, O.; Guo, L.; Lin, Z.; Qiu, B.; Chen, G. Electrochemiluminescence Biosensor for Folate Receptor Based on Terminal Protection of Small-Molecule-Linked DNA. *Biosens. Bioelectron.* **2014**, *58*, 226−231.
(16) Wu, L.; Wang, J.; Ren, J.; Li, W.; Qu, X. Highly Sensitive Electrochemiluminescent Cytosensing Using Carbon Nanodot@Ag Hybrid Material and Graphene for Dual Signal Amplification. *Chem. Commun.* **2013**, *49* (50), 5675−5677.
(17) Wei, X.; Lin, W.; Ma, N.; Luo, F.; Lin, Z.; Guo, L.; Qiu, B.; Chen, G. Sensitive Fluorescence Biosensor for Folate Receptor Based on Terminal Protection of Small-Molecule-Linked DNA. *Chem. Commun.* **2012**, *48* (49), 6184−6186.
(18) Ding, C.; Tian, Y. Gold Nanocluster-Based Fluorescence Biosensor for Targeted Imaging in Cancer Cells and Ratiometric Determination of Intracellular pH. *Biosens. Bioelectron.* **2015**, *65*, 183−190.
(19) Zhang, Y.; Liu, J.-M.; Yan, X.-P. Self-Assembly of Folate onto Polyethyleneimine-Coated CdS/ZnS Quantum Dots for Targeted Turn-On Fluorescence Imaging of Folate Receptor Overexpressed Cancer Cells. *Anal. Chem.* **2013**, *85* (1), 228−234.
(20) Zhao, J.; Hu, S.; Chen, X.; Zhang, B.; Wang, K.; Liu, X. A Colorimetric Method for the Detection of Folate Receptor Based on Terminal Protection-Assisted Cascade Signal Amplification. *Sens. Actuators, B* **2014**, *202*, 1243−1247.
(21) Jiao, L.; Xu, Z.; Du, W.; Li, H.; Yin, M. Fast Preparation of Polydopamine Nanoparticles Catalyzed by Fe^{2+}/H_2O_2 for Visible Sensitive Smartphone-Enabled Cytosensing. *ACS Appl. Mater. Interfaces* **2017**, *9* (34), 28339−28345.
(22) Cai, H.-H.; Pi, J.; Lin, X.; Li, B.; Li, A.; Yang, P.-H.; Cai, J. Gold Nanoprobes-Based Resonance Rayleigh Scattering Assay Platform: Sensitive Cytosensing of Breast Cancer Cells and Facile Monitoring of Folate Receptor Expression. *Biosens. Bioelectron.* **2015**, *74*, 165−169.
(23) Liu, S.; Cao, H.; Wang, Z.; Tu, W.; Dai, Z. Label-Free Photoelectrochemical Cytosensing via Resonance Energy Transfer Using Gold Nanoparticle-Enhanced Carbon Dots. *Chem. Commun.* **2015**, *51* (75), 14259−14262.
(24) Zhao, W.-W.; Xu, J.-J.; Chen, H.-Y. Photoelectrochemical Bioanalysis: the State of the Art. *Chem. Soc. Rev.* **2015**, *44* (3), 729−741.
(25) Fan, G.-C.; Han, L.; Zhu, H.; Zhang, J.-R.; Zhu, J.-J. Ultrasensitive Photoelectrochemical Immunoassay for Matrix Metalloproteinase-2 Detection Based on CdS:Mn/CdTe Cosensitized TiO_2 Nanotubes and Signal Amplification of SiO_2@Ab_2 Conjugates. *Anal. Chem.* **2014**, *86* (24), 12398−12405.
(26) Wang, L.; Han, D.; Ni, S.; Ma, W.; Wang, W.; Niu, L. Photoelectrochemical Device Based on Mo-Doped $BiVO_4$ Enables Smart Analysis of the Global Antioxidant Capacity in Food. *Chem. Sci.* **2015**, *6* (11), 6632−6638.
(27) Li, R.; Zhang, Y.; Tu, W.; Dai, Z. Photoelectrochemical Bioanalysis Platform for Cells Monitoring Based on Dual Signal Amplification Using in Situ Generation of Electron Acceptor Coupled with Heterojunction. *ACS Appl. Mater. Interfaces* **2017**, *9* (27), 22289−22297.
(28) Wang, M.; Ioccozia, J.; Sun, L.; Lin, C.; Lin, Z. Inorganic-Modified Semiconductor TiO_2 Nanotube Arrays for Photocatalysis. *Energy Environ. Sci.* **2014**, *7* (7), 2182−2202.
(29) Chen, D.; Zhang, H.; Li, X.; Li, J. Biofunctional Titania Nanotubes for Visible-Light-Activated Photoelectrochemical Biosensing. *Anal. Chem.* **2010**, *82* (6), 2253−2261.
(30) Kang, Q.; Yang, L.; Chen, Y.; Luo, S.; Wen, L.; Cai, Q.; Yao, S. Photoelectrochemical Detection of Pentachlorophenol with a Multiple Hybrid $CdSe_xTe_{1-x}/TiO_2$ Nanotube Structure-Based Label-Free Immunosensor. *Anal. Chem.* **2010**, *82* (23), 9749−9754.
(31) Zhao, W.-W.; Ma, Z.-Y.; Yan, D.-Y.; Xu, J.-J.; Chen, H.-Y. In Situ Enzymatic Ascorbic Acid Production as Electron Donor for CdS Quantum Dots Equipped TiO_2 Nanotubes: A General and Efficient Approach for New Photoelectrochemical Immunoassay. *Anal. Chem.* **2012**, *84* (24), 10518−10521.
(32) An, Y.; Tang, L.; Jiang, X.; Chen, H.; Yang, M.; Jin, L.; Zhang, S.; Wang, C.; Zhang, W. A Photoelectrochemical Immunosensor Based on Au-Doped TiO_2 Nanotube Arrays for the Detection of α-Synuclein. *Chem. - Eur. J.* **2010**, *16* (48), 14439−14446.
(33) Ma, H.; Fan, Q.; Fan, B.; Zhang, Y.; Fan, D.; Wu, D.; Wei, Q. Formation of Homogeneous Epinephrine-Melanin Solutions to Fabricate Electrodes for Enhanced Photoelectrochemical Biosensing. *Langmuir* **2018**, *34* (26), 7744−7750.
(34) Ma, H.; Yan, T.; Zhang, Y.; Gao, P.; Pang, X.; Du, B.; Wei, Q. A Biomimetic Mussel-Inspired Photoelectrochemical Biosensing Chip for the Sensitive Detection of CD146. *Analyst* **2015**, *140* (15), 5019−5022.
(35) Gabizon, A.; Shmeeda, H.; Horowitz, A. T.; Zalipsky, S. Tumor Cell Targeting of Liposome-Entrapped Drugs with Phospholipid-Anchored Folic Acid−PEG Conjugates. *Adv. Drug Delivery Rev.* **2004**, *56* (8), 1177−1192.
(36) Pan, D.; Turner, J. L.; Wooley, K. L. Folic Acid-Conjugated Nanostructured Materials Designed for Cancer Cell Targeting. *Chem. Commun.* **2003**, *19*, 2400−2401.
(37) Chan, P.; Kurisawa, M.; Chung, J. E.; Yang, Y.-Y. Synthesis and Characterization of Chitosan-g-Poly(Ethylene Glycol)-Folate as a Non-Viral Carrier for Tumor-Targeted Gene Delivery. *Biomaterials* **2007**, *28* (3), 540−549.
(38) Cui, M.; Song, Z.; Wu, Y.; Guo, B.; Fan, X.; Luo, X. A Highly Sensitive Biosensor for Tumor Maker Alpha Fetoprotein Based on Poly(Ethylene Glycol) Doped Conducting Polymer PEDOT. *Biosens. Bioelectron.* **2016**, *79*, 736−741.
(39) Wang, G.; Xu, Q.; Liu, L.; Su, X.; Lin, J.; Xu, G.; Luo, X. Mixed Self-Assembly of Polyethylene Glycol and Aptamer on Polydopamine Surface for Highly Sensitive and Low-Fouling Detection of Adenosine Triphosphate in Complex Media. *ACS Appl. Mater. Interfaces* **2017**, *9* (36), 31153−31160.
(40) Cheng, W.; Nie, J.; Xu, L.; Liang, C.; Peng, Y.; Liu, G.; Wang, T.; Mei, L.; Huang, L.; Zeng, X. pH-Sensitive Delivery Vehicle Based on Folic Acid-Conjugated Polydopamine-Modified Mesoporous Silica Nanoparticles for Targeted Cancer Therapy. *ACS Appl. Mater. Interfaces* **2017**, *9* (22), 18462−18473.
(41) Kang, Q.; Liu, S.; Yang, L.; Cai, Q.; Grimes, C. A. Fabrication of PbS Nanoparticle-Sensitized TiO_2 Nanotube Arrays and Their Photoelectrochemical Properties. *ACS Appl. Mater. Interfaces* **2011**, *3* (3), 746−749.
(42) Lee, H.; Dellatore, S. M.; Miller, W. M.; Messersmith, P. B. Mussel-Inspired Surface Chemistry for Multifunctional Coatings. *Science* **2007**, *318* (5849), 426.
(43) Balaur, E.; Macak, J. M.; Taveira, L.; Schmuki, P. Tailoring the Wettability of TiO_2 Nanotube Layers. *Electrochem. Commun.* **2005**, *7* (10), 1066−1070.

DOI: 10.1021/acsami.9b17630
ACS Appl. Mater. Interfaces 2020, 12, 1877−1884

(44) Wang, R.; Ma, H.; Zhang, Y.; Wang, Q.; Yang, Z.; Du, B.; Wu, D.; Wei, Q. Photoelectrochemical Sensitive Detection of Insulin Based on CdS/Polydopamine Co-Sensitized WO_3 Nanorod and Signal Amplification of Carbon Nanotubes@Polydopamine. *Biosens. Bioelectron.* **2017**, *96*, 345−350.

DOI: 10.1021/acsami.9b17630
ACS Appl. Mater. Interfaces 2020, 12, 1877−1884